

Effect of Inter-Electrode Spacing on Electrolyte Properties and Morphologies of Anodic TiO₂ Nanotube Array Films

Sorachon Yoriya

National Metal and Materials Technology Center, 114 Thailand Science Park, Paholyothin Road,
Klong 1, Klong Luang, Pathumthani 12120, Thailand
E-mail: sorachy@mtec.or.th

Received: 2 August 2012 / *Accepted:* 31 August 2012 / *Published:* 1 October 2012

This work presents the formation of TiO₂ nanotube arrays fabricated by electrochemical anodization of titanium in the fluoride-based diethylene glycol (DEG) electrolyte, with an aim towards elucidating how variation of inter-electrode spacing affects changes in electrolyte properties and corresponding morphological features of TiO₂ nanotube array films. Enlargement of nanotube morphologies of DEG fabricated nanotubes is attainable through a simplified synthesis technique and manipulation of electrolyte properties. Electrolyte conductivity and titanium concentration are found to drastically increase with decreasing anode-cathode separation. Resulting titania nanotube array morphologies also tends to increase significantly, particularly observed in intertubular spacing that increases by a factor of 15 as reducing the electrode spacing from 4.5 cm to 0.5 cm under a fixed electrolyte condition. Due to the combination effect of electrolyte properties and high field strength between the electrodes, the self-enlargement potential is believed to be a driving force for nanotube separation. The unique characteristic of discrete, well-separated nanotube structure is expected to extend and enhance the applications of anodic TiO₂ nanotube array films.

Keywords: TiO₂ nanotube arrays, electrochemical anodization, electrolyte conductivity, titanium concentration, inter-electrode spacing

1. INTRODUCTION

In recent years, TiO₂ nanotube arrays have attracted considerable attention due to their remarkable properties and utilities in potential applications. Self-organized, vertically oriented titania nanotube arrays have been found to possess outstanding properties enabling a variety of advanced applications including hydrogen gas sensor, [1-7] generation of hydrogen by water photoelectrolysis, [8-10] heterojunction solar cells, [2, 11-14] and biomedical uses. [15-21] Effects of synthesis parameters on structures of self-organized TiO₂ nanotube arrays have been widely studied with many

attempts to cover the parameter significance, enabling precise control of nanotube morphological features and their corresponding properties.

The field of electrochemical anodization of titanium has grown rapidly through several fabrication generations using different electrolyte systems, starting from aqueous to non-aqueous/polar organic electrolytes in which a wide variety of synthesis chemistries, competition reactions of localized chemical dissolution with field-assisted oxidation and dissolution take place, allowing precisely ordered, unique characteristics of TiO₂ nanotube arrays to be achieved. [14, 22-24] The electrolyte nature and its composition are considered as the key factors governing the nanotube growth process. Polar organic electrolytes, such as formamide (FA), dimethyl sulfoxide (DMSO), N-methylformamide (NMF), dimethyl formamide (DMF), and ethylene glycol (EG), has attracted more attention and become the most popular anodization electrolyte medium during the past recent years. Approaches to achieving the very long tube length and the large pore size have been extensively reported using those organic electrolytes. [11, 25-30] A wide variation of nanotube-to-nanotube spacing is known that could be obtained in diethylene glycol (DEG) electrolyte.[31-33] Such unique characteristic of DEG fabricated titania nanotubes has been attracted increasing attention in biomedical applications, allowing for enhancing cellular adhesion and increasing protein adsorption and loading of multiple sized drugs. [34-37]

Since selection of electrolyte medium for anodization is critically important, manipulating the anodization conditions is even more restricted. Explanation in details about growth mechanisms of TiO₂ nanotube arrays is an essential need. To date, a particular focus on driving force for self-ordering, nanotube array orientation, and especially nanotube separation, to the best of our knowledge, is not fully understood. A precise control of tube-to-tube spacing is still a great challenge. The pore formation of TiO₂ film have been widely proposed through several models and solution matrix. Many attempts have been made toward elucidating the growth mechanisms of the two most intriguing features of TiO₂ nanotube array architectures: the hexagonally close-packed and the well-discrete, freely self-standing structures of nanotubes. [23, 38-41] The distinct, multipodal hollow structure of titania nanotubes has been recently reported and observed in DEG electrolyte with a proposed mechanism of capillary forces explaining the phenomena of bending and bunching of nanotubes; [29] however, driving force for the tube cell separation has been rarely mentioned.

Herein, the work reports on the fabrication of TiO₂ nanotube array films in diethylene glycol (DEG) electrolyte with enlarged nanotube morphologies achieved by a simplified anodization technique. The work details how the control distance between anode and cathode electrodes has significant effects on the tube morphological parameters, particularly the tube-to-tube spacing. Electrolyte properties in terms of conductivity and titanium concentration have been investigated and studied their effects on the relating morphologies of titania nanotube array films.

2. EXPERIMENTAL

Titanium foils (0.25 mm, 99.7%, Sigma-Aldrich), cut in 1 cm × 2.5 cm in size, were cleaned with acetone, degreased with soap and deionized water following by iso-propanol prior to anodization.

In the experiment, the electrolyte condition selected in this work is diethylene glycol (DEG, 99.7 %, Sigma-Aldrich) containing 2 % hydrofluoric acid (HF, 48 % solution, Merck), with no other additives employed. Potentiostatic anodization was performed at room temperature of about 23 °C, using a two-electrode electrochemical cell with a platinum foil as a counter electrode. Configuration and size of the platinum foil used in this work is as same as the titanium anode electrode. The Pt foil counter electrode was set in a good parallel with a Ti foil working electrode to keep constant the flux lines or the uniform current distribution between the two electrodes. Thus, the enhanced effect of non-uniform total resistance along the path will be neglected. The anode-cathode separation was varied from 0.5 cm to 4.5 cm. The anodization condition was held fixed using the applied voltage at 60 V and 24-h anodization duration. After anodization, the anodized films were rinsed with iso-propanol and blow-dried with nitrogen gas prior to morphological study. Morphologies of the titania nanotube array films were characterized by field emission scanning electron microscope (FE-SEM, Leo 1530). Conductivity of the anodized electrolytes was measured at room temperature using a conductivity meter (YSI 3200, Cole-Parmer). The concentration of titanium dissolving in the electrolytes after anodization was investigated by inductively coupled plasma atomic emission spectrometry (ICP-AES, Perkin-Elmer Optima 5300 ICP). Both measured conductivity and titanium concentration were normalized to the value per anodized area of titanium foil of 3.0 cm².

3. RESULT AND DISCUSSION

3.1 Electrolyte Properties

The conductivities and titanium concentrations measured from the anodized electrolyte as a function of inter-electrode (Pt-Ti) spacing are shown in Table 1. As a function of inter-electrode spacing, plots of the electrolyte conductivity and the titanium concentration are shown in Figure 1 (a) and (b); a linear relation of these two parameter can be observed in Figure 1 (c). In Figure 1 (a) and (b), the trend that the conductivity increases with the decreased inter-electrode spacing is similar to that observed for the titanium concentration. A significant change in those slopes is clearly seen for the small electrode separation ranging between 0.5 cm and 1.0 cm. As clearly seen in Figure 1 (c), the conductivities of such closer electrode spacing lies in the higher regime ($> 60 \mu\text{S cm}^{-1}$). Whereas for the large electrode spacings ranging between 2.0 cm to 4.5 cm, the measured conductivities are in the lower region, which is less than $60 \mu\text{S cm}^{-1}$.

With a constant anodized area of Ti sample of 3.0 cm², the measured electrolyte conductivity and titanium concentration values are in the range of $120 \mu\text{S cm}^{-1}$ and 1200 ppm, respectively. The nominal conductivity range of $120 \mu\text{S cm}^{-1}$ is comparatively lower than those observed for other organic electrolytes. [25, 27] The low conductivity of DEG electrolyte has been remarked upon important combined factors: (i) the high viscosity of DEG and a consequent concomitant low ionic mobilities; (ii) low concentration of ionic charge carriers due to low dissociation of the hydrofluoric weak acid; and (iii) large hydrodynamic radius of dissociated ions due to the solvation phenomena by water and DEG molecules. [29, 39]

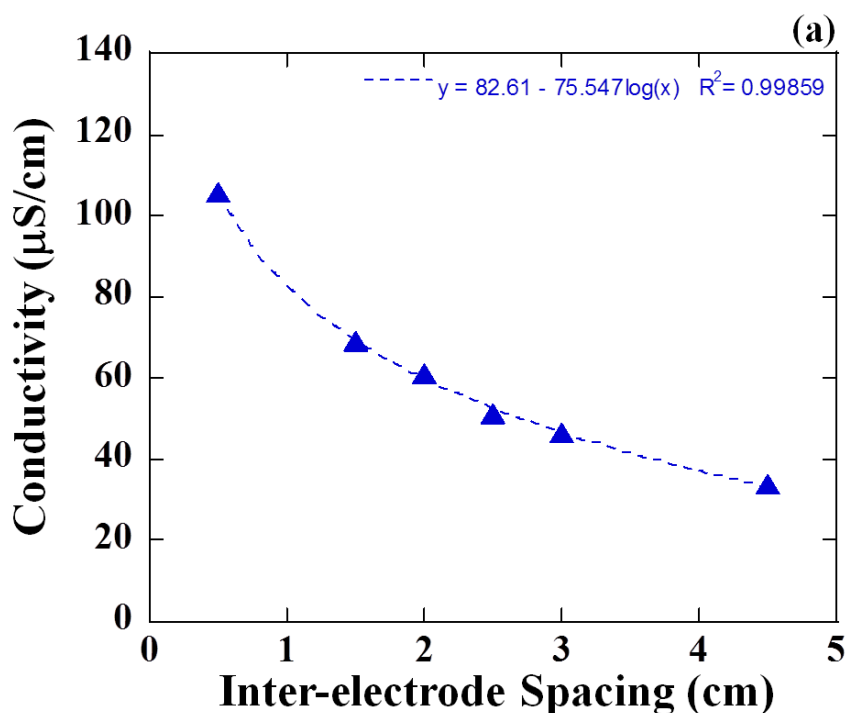
Table 1. Conductivities and titanium concentrations of the DEG–2.0 % HF electrolytes anodized at 60 V for 24 h using different inter-electrode spacing, with those values normalized per the anodized Ti area of 3.0 cm².

Inter-electrode spacing (cm)	Conductivity (μS/cm)	Ti concentration (ppm)
0.5	105.5	1044.6
1.5	69.1	712.6
2.0	61.0	460.0
2.5	51.0	510.0
3.0	46.3	407.5
4.5	34.0	459.6

The plots in Figure 1 (c) indicate that the electrolyte conductivity is proportional to the concentration of titanium ions dissolving into the electrolyte during anodization, [39] when the increased conductivity makes a large proportion of applied anodization voltage available for the anodization process, manifesting itself in a high density of anodic oxidation reactions including titanium dissolution. This relationship is in a good agreement with this following equation (equation 1) that the electrolyte conductivity κ is proportional to the concentrations c of the constituent ions (ion i) for the dilute electrolyte solutions. [42]

$$\kappa = \sum |Z_i| \mathcal{F} u_i c_i = \sum \lambda_i c_i \tag{1}$$

Where Z_i is the ion i charge number, \mathcal{F} is Faraday constant, u_i is the electric mobility of ion i and the proportionality constant λ_i is the ionic conductivity or the molar conductivity of ion i .



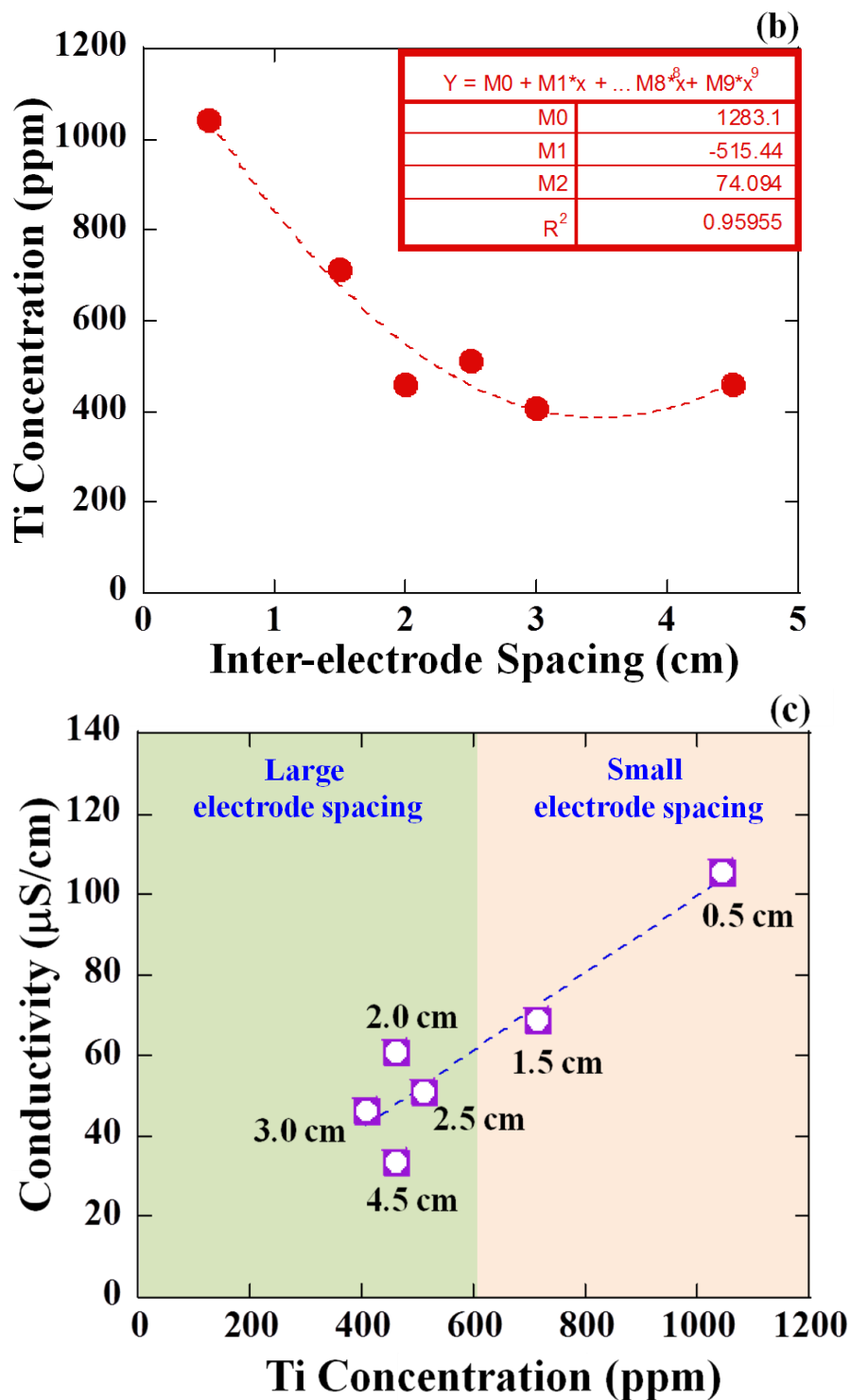


Figure 1. (a) Conductivity and (b) titanium concentration values measured from the anodized DEG–2.0 % HF electrolytes (60 V and 24 h) plotted against inter-electrode spacing. (c) A plot of electrolyte conductivity vs. titanium concentration using those data shown in Table 1.

Due to the electrode kinetics, the closer inter-electrode spacing could facilitate the electrode reactions, promoting the oxide growth process and the chemical dissolution simultaneously; the large titanium dissolution is hence observed. While the higher conductivity due to the greater supply of free

ions in the electrolyte in turn induces more charges to be formed on the oxide layer, improving extraction of Ti^{4+} ions. [43] Thus, a greater concentration of titanium ion dissolving in the electrolyte was obtained. A simultaneous effect the oxide dissolution significantly enhanced due to the improved conductivity could in turn lead to the greater titanium concentration.[39] The situation can be expressed as these following reactions, competitive reactions between chemical dissolution (reaction 2) and electrochemical anodic oxidation (reaction 3). [23, 44] Further, changes in electrode microstructure, electrolyte contamination, and control of mass transport to the electrode can all contribute to variations in electrode reactions.[45]



3.2 Morphological Study

Table 2 shows variation of nanotube morphological features including pore sizes at the top and the bottom of nanotube arrays, wall thickness, and intertubular spacing achieved as a function of electrode separation. The plots of those values in

Table 2 are demonstrated in Figure 2.

Table 2. Top pore size, bottom pore size, wall thickness, intertubular spacing, and the calculated values of improved morphology factor (IMF) of TiO_2 nanotube arrays obtained at different inter-electrode spacings. All conditions were anodized in DEG-2.0 % HF electrolytes, 60 V for 24 h.

Inter-electrode spacing (cm)	Top pore size (nm)	$\text{IMF}_{\text{Top pore size}}$	Bottom pore size (nm)	$\text{IMF}_{\text{Bottom pore size}}$	Wall thickness (nm)	$\text{IMF}_{\text{Wall thickness}}$	Intertubular spacing (nm)	$\text{IMF}_{\text{Intertubular spacing}}$
0.5	192.0 ± 30.6	4.69	156.9 ± 24.4	5.16	65.1 ± 6.4	5.05	155.7 ± 14.5	15.1
1.5	172.5 ± 17.8	4.22	132.7 ± 22.8	4.37	51.4 ± 3.0	3.98	86.4 ± 18.2	8.39
2.0	141.5 ± 17.7	3.46	102.0 ± 15.6	3.36	38.6 ± 3.9	2.99	76.6 ± 11.0	7.44
2.5	125.9 ± 19.4	3.08	96.6 ± 19.1	3.18	36.4 ± 3.5	2.82	67.8 ± 19.8	6.58
3.0	93.3 ± 11.6	2.28	59.3 ± 14.7	1.95	30.2 ± 3.0	2.34	39.9 ± 14.2	3.87
4.5	40.9 ± 6.5	1.00	30.4 ± 9.2	1.00	12.9 ± 1.6	1.00	10.3 ± 2.6	1.00

The nanotube growth is strictly controlled by the field assisted anodization process where the electric field strength is the most important parameter governing the nanopores. [30, 38, 46] The bottom pore growth is determined by the ionic transports of metal cations and oxygen anions through the oxide layer at the metal/oxide or oxide/electrolyte interfaces.[46, 47] At the minimum separation of 0.5 cm, the increased electrolyte conductivity due to the large titanium ion dissolving into the electrolyte in turn makes a large contribution to the electrochemical oxidation and dissolution reactions, facilitating the growth process and thus dominating the oxide formation. It is clearly observed in Figure 2 that the nanotube morphologies increased in the similar behavior as reducing the electrode separation. The result obtained in this work indicates that large pore size, thicker tube wall, and wider tube separation could be achieved by simply manipulating the anodization technique.

However, an interesting point was made; that is, increment of the top pore size with the electrode spacing tends to deviate from that of the bottom pore size, especially at the inter-electrode positions between 0.5 and 2.5 cm; see the light blue color highlighted in Figure 2. The distance between Pt and Ti electrodes normally used in either aqueous or non-aqueous electrolytes is 2.0 cm. [48, 49] The observation gives a good suggestion to this point of view that, under a fixed anodization condition, even a slight change in inter-electrode spacing within this range could possibly produce the tapered morphology of nanotubes.

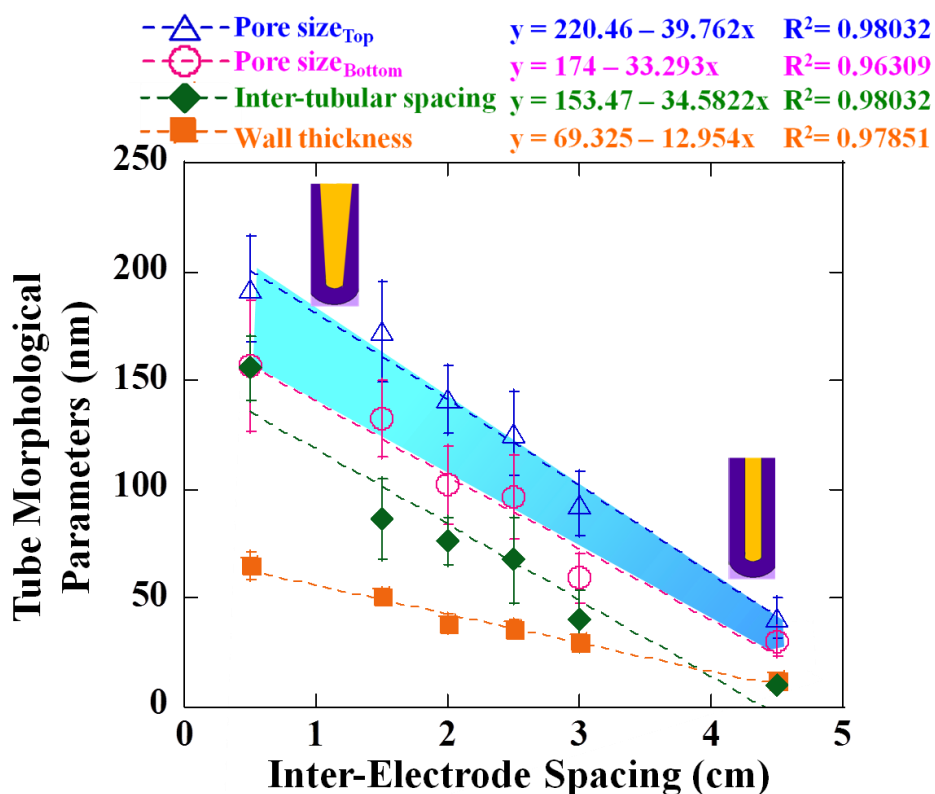


Figure 2. Variation of Nanotube morphological parameters as a function of inter-electrode spacing. Anodizations of Ti foil samples were performed in DEG–2.0% HF electrolyte at 60 V for 24 h anodization.

The tapered structure is ascribed to the well-known dependence of pore diameter on chemical dissolution that proceeds to a relatively greater extent at the top of nanotube layer, leading to the formation of conical structure nanotubes over the course of anodization. [23, 50] The small electrode separation is believed to predominantly contribute the large chemical dissolution to the process in which the magnitude of flux leading a severe mass transport between electrodes plays a key role. [30, 32] Under the same condition of DEG-2.0 % HF electrolytes, 60 V and 24 h, variation of inter-electrode spacing showed no effect on the resulting film thickness; the nanotube array length of $\sim 3 \mu\text{m}$ was obtained for all conditions. In

Table 2, degree of morphology enlargement was also determined in terms of the so-called improved morphology factor (IMF)— the ratio of tube morphology parameter obtained at each inter-electrode spacing divided by the tube morphology value obtained at the largest electrode spacing of 4.5 cm. Over a reducing range of 4.5-to-0.5 cm, the IMF values of pore sizes and wall thickness were found to increase by a factor of 5. Interestingly for the intertubular spacing, its IMF value was found to be much larger with the increased factor of 15. The large deviation of the IMF-electrode distance plot is obviously observed in Figure 3. This result clearly indicates that minimizing the electrode distance towards the minimum position has shown its significant effect specifically on the tube-to-tube spacing parameter. It could be understood from this observation that the self-enlargement potential, mainly governed by the combination effect of electrolyte properties and the high field strength between the electrodes, is a driving force for the nanotube separation.

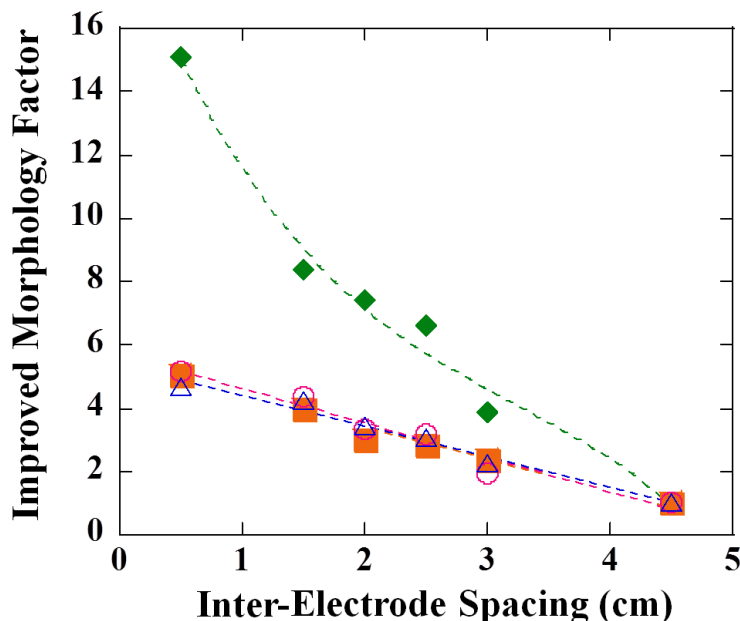


Figure 3. A plot of inter-electrode spacing vs. improved morphology factor of morphological parameters of TiO_2 nanotube array films grown in DEG–2.0% HF electrolyte, 60 V and 24 h anodization.

The top view FESEM images of the resulting TiO₂ nanotube arrays obtained from different inter-electrode spacings are shown in Figure 4. Unique characteristics of DEG fabricated nanotubes have been confirmed by the achievement of well-separated nanotubes as seen in all varying conditions. Compared to the condition of 4.5 cm, larger pore size and smaller number of nanotubes are seen more clearly for the 0.5 cm condition. Due to a very high competitive oxide growth in this electrolyte condition, some pore channels with relatively slower growth rate could probably stop expansion, leaving some ungrown pores existing in between nanotubes; as a result, the less number of nanotubes is seen. While for the case where the counter electrode (Pt) is far removed from the working electrode (Ti), a significant decrease in pore size and a large increase in number of titania nanotubes are obtained. The apparent decrease in pore diameter is probably due to the significant IR drop along the current path in the electrolyte reducing the field strength at the anode electrode.[30, 48, 51]

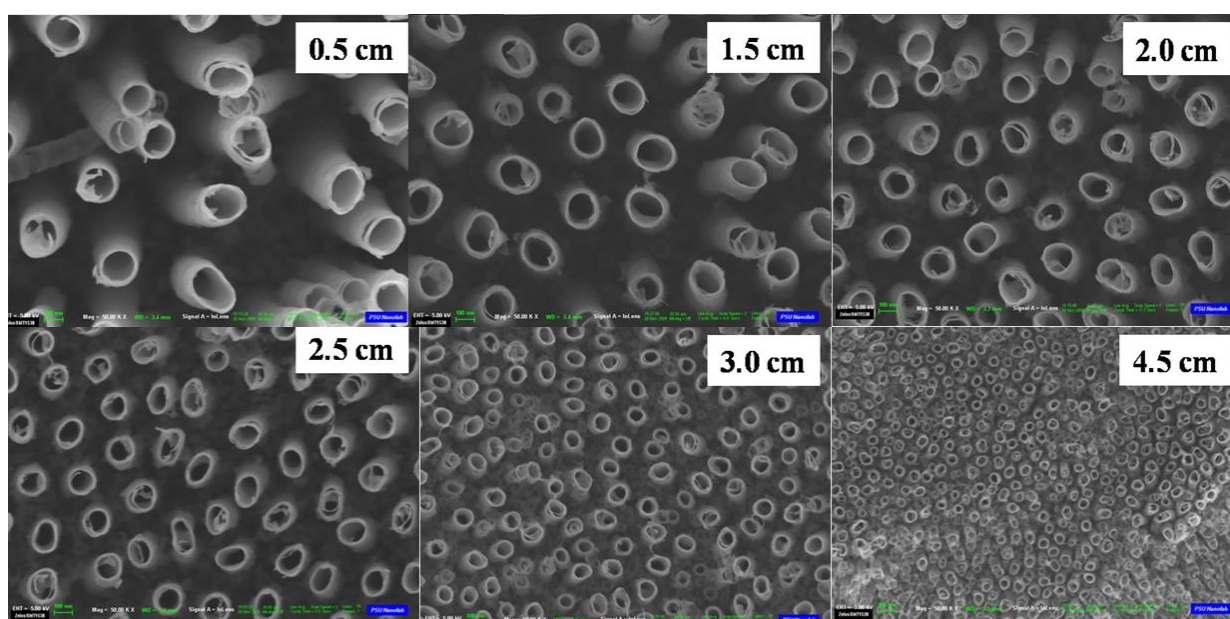


Figure 4. Top view FESEM images of TiO₂ nanotube array films anodized in DEG–2.0 % HF electrolytes at 60 V and for 24 h using different inter-electrode spacings: 0.5, 1.5, 2.0, 2.5, 3.0, and 4.5 cm. The scale bar shown in all figures is 100 nm.

4. CONCLUSION

In summary, this study provided a specific insight into the effect of inter-electrode spacing on the resulting electrolyte properties and corresponding morphologies of titania nanotube array films fabricated in diethylene glycol electrolyte. The relations between inter-electrode spacing and electrolyte properties in terms of conductivity and titanium concentration, and morphological parameters were established. The electrolyte conductivity and titanium concentration were found to strongly depend upon the electrode spacing, with the closer electrode spacings reflecting high conductivity and high titanium concentration. Enlargement of pore diameters, wall thickness, and

inter-tubular spacing could be achieved by simply reducing the inter-electrode spacing under a fixed condition of DEG–2%HF electrolyte. Further interesting result revealed that the small electrode separation showed the most significant effect on the intertubular spacing parameter that increased by a factor of 15 as decreasing the anode-cathode spacing from 4.5 cm to 0.5 cm, giving a good indication of a specific effect of inter-electrode spacing on the nanotube separation process. Due to the combination effect of the electrolyte properties and the high field strength between the electrodes, it is believed that the self-enlargement potential is a driving force for the nanotube separation.

ACKNOWLEDGEMENTS

S. Yoriya acknowledges the National Metal and Materials Technology Center (MTEC), Thailand, for providing facilities and research funding through the Ceramics Technology Research Unit. The author also thank Dr. Henry Gong for helpful ICP-AES analysis. Partial support of this work through the Material Research Institute (MRI), Department of Materials Science and Engineering, the Pennsylvania State University USA, is also gratefully acknowledged.

References

1. C. A. Grimes, *J. Mater. Chem.* 17 (2007) 1451
2. M. Paulose, K. Shankar, O. K. Varghese, G. K. Mor, B. Hardin and C. A. Grimes, *Nanotechnology* 17 (2006) 1446
3. O. K. Varghese, X. P. Yang, J. Kendig, M. Paulose, K. F. Zeng, C. Palmer, K. G. Ong and C. A. Grimes, *Sens. Lett.* 4 (2006) 120
4. O. K. Varghese, G. K. Mor, C. A. Grimes, M. Paulose and N. Mukherjee, *J. Nanosci. Nanotechnol.* 4 (2004) 733
5. G. K. Mor, O. K. Varghese, M. Paulose and C. A. Grimes, *Sens. Lett.* 1 (2003) 42
6. O. K. Varghese, D. W. Gong, M. Paulose, K. G. Ong and C. A. Grimes, *Sens. Actuators B-Chemical* 93 (2003) 338
7. O. K. Varghese, D. W. Gong, M. Paulose, K. G. Ong, E. C. Dickey and C. A. Grimes, *Adv. Mater.* 15 (2003) 624
8. G. K. Mor, K. Shankar, M. Paulose, O. K. Varghese and C. A. Grimes, *Nano Lett.* 5 (2005) 191
9. M. Paulose, G. K. Mor, O. K. Varghese, K. Shankar and C. A. Grimes, *J. Photochem. Photobiol. a-Chemistry* 178 (2006) 8
10. O. K. Varghese, M. Paulose, K. Shankar, G. K. Mor and C. A. Grimes, *J. Nanosci. Nanotechnol.* 5 (2005) 1158
11. K. Shankar, G. K. Mor, H. E. Prakasam, S. Yoriya, M. Paulose, O. K. Varghese and C. A. Grimes, *Nanotechnology* 18 (2007) 065707; 11 pages
12. G. K. Mor, K. Shankar, M. Paulose, O. K. Varghese and C. A. Grimes, *Nano Lett.* 6 (2006) 215
13. K. Zhu, N. R. Neale, A. Miedaner and A. J. Frank, *Nano Lett.* 7 (2007) 69
14. G. K. Mor, O. K. Varghese, M. Paulose, K. Shankar and C. A. Grimes, *Sol. Energy Mater. Sol. Cells* 90 (2006) 2011
15. K. C. Popat, L. Leoni, C. A. Grimes and T. A. Desai, *Biomaterials* 28 (2007) 3188
16. L. Peng, A. D. Mendelsohn, T. J. LaTempa, S. Yoriya, C. A. Grimes and T. A. Desai, *Nano Lett.* 9 (2009) 1932
17. L. Peng, A. J. Barczak, R. A. Barbeau, Y. Y. Xiao, T. J. LaTempa, C. A. Grimes and T. A. Desai, *Nano Lett.* 10 (2010) 143
18. K. S. Brammer, S. Oh, C. J. Cobb, L. M. Bjursten, H. van der Heyde and S. Jin, *Acta Biomater.* 5 (2009) 3215

19. J. Park, S. Bauer, K. A. Schlegal, F. W. Neukam, K. von der Mark and P. Schmuki, *Small* 5 (2009) 666
20. N. Swami, Z. Cui and L. S. Nair, *J. Heat Transfer* 133 (2011) 034002
21. S. C. Roy, M. Paulose and C. A. Grimes, *Biomaterials* 28 (2007) 4667
22. D. Gong, C. A. Grimes, O. K. Varghese, W. C. Hu, R. S. Singh, Z. Chen and E. C. Dickey, *J. Mater. Res.* 16 (2001) 3331
23. G. K. Mor, O. K. Varghese, M. Paulose, N. Mukherjee and C. A. Grimes, *J. Mater. Res.* 18 (2003) 2588
24. C. A. Grimes and G. K. Mor, *TiO₂ Nanotube Arrays: Synthesis, Properties, and Applications*, Springer, New York (2009)
25. H. E. Prakasam, K. Shankar, M. Paulose, O. K. Varghese and C. A. Grimes, *J. Phy. Chem. C* 111 (2007) 7235
26. M. Paulose, H. E. Prakasam, O. K. Varghese, L. Peng, K. C. Popat, G. K. Mor, T. A. Desai and C. A. Grimes, *J. Phy. Chem. C* 111 (2007) 14992
27. M. Paulose, K. Shankar, S. Yoriya, H. E. Prakasam, O. K. Varghese, G. K. Mor, T. A. Latempa, A. Fitzgerald and C. A. Grimes, *J. Phy. Chem. C B* 110 (2006) 16179
28. S. P. Albu, A. Ghicov, S. Aldabergenova, P. Drechsel, D. LeClere, G. E. Thompson, J. M. Macak and P. Schmuki, *Adv. Mater.* 20 (2008) 4135
29. A. Mohammadpour, P. R. Waghmare, S. K. Mitra and K. Shankar, *ACS Nano* 4 (2010) 7421
30. J. M. Macak, H. Hildebrand, U. Marten-Jahns and P. Schmuki, *Journal of Electroanal. Chem.* 621 (2008) 254
31. S. Yoriya, G. K. Mor, S. Sharma and C. A. Grimes, *J. Mat. Chem.* 18 (2008) 3332
32. S. Yoriya and C. A. Grimes, *Langmuir* 26 (2010) 417
33. A. Mohammadpour and K. Shankar, *J. Mat. Chem.* 20 (2010) 8474
34. B. S. Smith, S. Yoriya, L. Grissom, C. A. Grimes and K. C. Popat, *J. Biomed. Mater. Res. Part A* 95A (2010) 350
35. K. C. Popat, M. Eltgroth, T. J. LaTempa, C. A. Grimes and T. A. Desai, *Biomaterials* 28 (2007) 4880
36. K. C. Popat, M. Eltgroth, T. J. La Tempa, C. A. Grimes and T. A. Desai, *Small* 3 (2007) 1878
37. K. Gulati, S. Ramakrishnan, M. S. Aw, G. J. Atkins and D. M. Findlay and D. Losic *Acta Biomater.* 8 (2012) 449
38. Z. Su and W. Zhou, *Adv. Mater.* 20 (2008) 3663
39. S. Yoriya and C. A. Grimes, *J. Mat. Chem.* 21 (2011) 102
40. S. Berger, H. Tsuchiya and P. Schmuki, *Chem. Mater.* 20 (2008) 3245
41. A. Ghicov, H. Tsuchiya, J. M. Macak and P. Schmuki, *Electrochem. Commun.* 7 (2005) 505
42. K. Izutsu, *Electrochemistry in Nonaqueous Solutions*, Wiley-VCH, New York (2002)
43. K. Shankar, G. K. Mor, A. Fitzgerald and C. A. Grimes, *J. Phy. Chem. C* 111 (2007) 21
44. S. Yoriya, M. Paulose, O. K. Varghese, G. K. Mor and C. A. Grimes, *J. Phy. Chem. C* 111 (2007) 13770
45. G. Prentice, *Electrochemical Engineering Principles*, Prentice Hall, New Jersey (1991)
46. J. W. Diggle, T. C. Downie and C. W. Goulding, *Chem. Rev.* 69 (1969) 365
47. K. Yasuda and P. Schmuki, *Electrochim. Acta* 52 (2007) 4053
48. M. Noranimuti, A. A. Dzilal and J. O. Dennis, *J. Eng. Sci. Technol.* 3 (2008) 163
49. Y. Alivov, M. Pandikunta, S. Nikishin and Z. Y. Fan, *Nanotechnology* 20 (2009) 225602 (6pp)
50. S. Berger, J. Kunze, P. Schmuki, A. T. Valota, D. J. LeClere, P. Skeldon and G. E. Thompson, *J. Electrochem. Soc.* 157 (2010) C18
51. L. Sun, S. Zhang, X. W. Sun and X. He, *J. Electroanal. Chem.* 637 (2009) 6